Title

THE REACTION pn -9. ppir"" AND N*(l470) PRODUCTION AT 6 GeV/c

Authors

Gage, W.
Colton, E.
Chinowsky, W.

Publication Date

1970-09-01

Submitted to Physical
Review Letters

UCRL-20106
Preprint
c.2

THE REACTION $pn \rightarrow pp\pi^-$ AND N*(1470) PRODUCTION AT 6 GeV/c

W. Gage, E. Colton and W. Chinowsky

September 1970

AEC Contract No. W-7405-eng-48

UCRL-20106

LAWRENCE RADIATION LABORATORY
UNIVERSITY of CALIFORNIA BERKELEY

THE REACTION pn $\rightarrow pp\pi^-$ and N*(1470) PRODUCTION AT 6 GeV/c*

W. Gage, E. Colton and W. Chinowsky

Lawrence Radiation Laboratory
University of California, Berkeley, California 94720

September 1970

ABSTRACT

A search for N* (1470) production has been made among the 904 selected examples of the reaction pd $\rightarrow pp\pi^-(p_{sp})$ obtained in a bubble chamber exposure at 5.9 GeV/c incident momentum. The peripheral data are in good agreement with the predictions of a single pion exchange model. At most 5% of the events are attributable to N* (1470) production by some other mechanism.

The rather convincing evidence for existence of a T = 1/2, J = 1/2 nucleon isobar at mass of about 1450 MeV/c^2, revealed both in missing-mass spectrometer experiments[1] and in phase shift analyses of pion-nucleon elastic scattering,[2] has stimulated many searches for production of the resonance in bubble chamber experiments. Since observations in bubble chambers provide detailed information about all particles involved in production and decay, study of such events should provide understanding of the production mechanism. The particularly interesting feature of the process is the very sharp decrease of production cross section with momentum transfer, not consistent with a single-pion-exchange mechanism. The reaction pn $\rightarrow pp\pi^-$ is especially suitable for a production experiment since only charged particles are involved so that full kinematical constraints can be imposed in fitting. Further, the usual dominance of the final state interactions by the Δ (1238) is less strong here since there is no pure T = 3/2 nucleon-pion system produced. Indeed, perhaps the most compelling evidence for production of N* (1470) has been obtained in pd reactions at 7.0 GeV/c incident momentum reported by A. Shapira et al.[3]

We present here the results of an experiment with 5.9 GeV/c protons incident on the LRL 72" liquid deuterium bubble chamber which give no clear indication at all of N* (1470) production in the reaction $pd \rightarrow pp\pi^- (p_{sp})$, where p_{sp} indicates a "spectator" proton.

To provide the data, all three-prong events and four-prong events with at least one stopping positive track were measured on 70,000 frames of a total exposure of 100,000 photographs. On the average there were 12 incident protons. The 20,000 events measured were kinematically fitted, using the TVGP-SQUAW program system to the reactions

$$pd \rightarrow pp\pi^- \, p_{sp} \qquad (1)$$

$$pd \rightarrow p\pi^+\pi^- n \, p_{sp} \qquad (2)$$

$$pd \rightarrow pp\pi^-\pi^0 \, p_{sp} \qquad (3)$$

$$pd \rightarrow pd\pi^+\pi^- \qquad (4)$$

The fitting procedure uses as starting values for the spectator (p_{sp}) momentum the measured value for four-prong events. Spectator protons in the three-prong events have momenta too small ($\lesssim 80$ MeV/c) to produce an observable track. For such events, the starting values of "measured" momentum components were taken to be 0 ± 30 MeV/c for components in a plane perpendicular to the chamber's magnetic field direction and 0 ± 40 MeV/c for the vertical component. Events were accepted only if the inferred projected length of the spectator track was consistent with the observed, within the errors. In practice this meant a tolerance of ± 1.0 mm inconsistency between the "fitted" length and the observed. Momentum uncertainties in fact were great enough to absorb such variations without significantly affecting the χ^2 of the fit. A total of 1245 events were obtained fitting reaction (1) and satisfying incident beam and fiducial volume requirements. Further observation on the scanning table, to determine consistency of bubble density resulted in the elimination of 188 of these.

Ambiguities, mostly between fits to (1) and (3), π^0 production, were in all cases decided in favor of the higher constraint fit of the single-pion production reaction. There resulted 1057 events in the sample considered to be examples of process (1). To check scanning efficiencies and possible biases in the measurements, a smaller number, 20% of the total was rescanned and failed events remeasured. In none of the distributions to be presented was any evidence of detectable bias uncovered in comparing the two groups of data. The final sample, after excluding all events with confidence level $<$ 2%, is 904 events, of which 686 are three-prongs and 218 have a visible spectator.

The spectator track is defined as the lowest momentum track which, further, must be a stopping track. Evidence for the appropriateness of this procedure is provided by the distributions in spectator momentum and angle in the lab system, seen in Figs. 1 (a) and 1 (b) respectively. Included in those plots are the inferred momenta and angles obtained in the fitting procedure for the three-prong events with non-visible spectator. The momentum distribution is in good agreement with the square of the Hulthén momentum-space wave function[4] (normalized to the total number of events), shown superimposed on the experimental histogram of Fig. 1 (a). Deviations from isotropy in the angular distribution result from dependence of the flux factor[5] on the direction of motion of the initial state neutron. As seen in Fig. 1 (b) the angular distribution is also in excellent agreement with the isotropic distribution modified by this factor, shown together with the observed distribution. Thus the events are considered, for further analysis, to result from proton-neutron interactions, viz $pn \rightarrow pp\pi^-$ with the initial-state neutron given a momentum opposite to that of the spectator proton.

The events are strongly peripheral, as can be seen from the momentum-transfer distributions of Figs. 2 (a) and 2 (b).

We plot the momentum transfer from the target neutron to the slower of the two protons, (p_s),

$$t_{p_s} = (E_{p_s} - E_n)^2 - (\vec{P}_{p_s} - \vec{P}_n)^2 \qquad (5a)$$

and from the incident proton to the faster proton, (p_f) as observed in the lab. system,

$$t_{p_f} = (E_{p_f} - E_p)^2 - (\vec{P}_{p_f} - \vec{P}_p)^2 \qquad (5b)$$

where the E's and $\vec{P}$'s are the lab energies and momenta of the particles specified by the subscripts. Both distributions are strongly peaked at low momentum transfer, suggesting a single-particle-exchange mechanism. Distributions in effective masses,

$$M(p_f\pi^-) = \left[(E_{p_f} + E_{\pi^-})^2 - (\vec{P}_{p_f} + \vec{P}_{\pi^-})^2 \right]^{1/2} \qquad (6a)$$

and

$$M(p_s\pi^-) = \left[(E_{p_s} + E_{\pi^-})^2 - (\vec{P}_{p_s} + \vec{P}_{\pi^-})^2 \right]^{1/2} \qquad (6b)$$

are presented in Figs. 2 (c) and 2 (d) respectively. These, while clearly showing dynamical effects, do not demonstrate any particularly significant sharp peaking. In particular the variation with $M(p_s\pi^-)$ is in disagreement with that of Shapira et al.[3] in the absence of a peak near 1450 MeV/c^2, there being just a small departure from monotonic decrease in that region. We show below that but for small residual effects, these distributions are in good agreement with single-pion-exchange expectations.

To confront the data with pion-exchange model predictions we first restrict the sample to those 538 events with $|t_{p_s}| < 0.4$ (GeV/c)^2. The shaded histograms in Fig. 2 and the distributions in Fig. 3 represent those events with $|t_{p_s}| < 0.4$ (GeV/c)^2. The curves are described below. At the pion-nucleon energies relevant here, the diagram with π^- exchange contributes six times more to the total intensity than the corresponding diagram with π^0 exchange.

Theoretical curves drawn in Figs. 2 and 3 were obtained from a sample of 30,000 events generated, using Monte-Carlo methods, according to the production amplitudes of the two diagrams, added incoherently. Kinematical form factors of the Dürr-Pilkuhn type[6] were used to modify the pole equation[7] for use in the physical region of t. These form factors were obtained in analyses[8-10] of πp, Kp, $\bar{p}p$ and pp inelastic reactions over a large range of incident beam momenta. In addition, we have included the weakly t - dependent factor[11]

$$G^2(t) = \left[\frac{2.3 - \mu^2}{2.3 + t}\right]^2 \qquad (7)$$

in the expression for $d^2\sigma/dM\,dt$, which Wolf[8] found necessary. In (7) μ is the pion mass. The $\pi^- p$ elastic and charge-exchange differential cross sections which are required in the calculations were constructed from the "CERN" phase shifts.[12]

Comparisons of the model predictions with the data are shown in the shaded distributions of Figs. 2 (b) - 2 (d) as well as those of Fig. 3. Figures 3 (a) (3 (b)) show the distributions in the cosine of the angle between the initial proton (neutron) and the outgoing p_f (p_s) as seen in the $p_f\pi^-$ ($p_s\pi^-$) rest systems. The corresponding Treiman-Yang (azimuthal) angles Φ_{p_f} and Φ_{p_s} are displayed in Figs. 3 (c) and 3 (d) respectively, while the momentum transfer to the π^-, $t_{p\pi^-}$ and $t_{n\pi^-}$ are plotted in Figs. 3 (e) and 3 (f) respectively. The observed distributions are in excellent agreement with the pion-exchange model predictions, normalized to a total sample of 538 events. We find, then, that for those events with "small" momentum transfer, $|t_{p_s}| < 0.4$ (GeV/c)^2, no additional resonance production mechanism need be invoked.

To help isolate possible N* (1470) production events in the $p_s\pi^-$ configuration, which in fact is the one in which Shapira et al.[3] observed large "anomalous" N* (1450) production, events were selected satisfying criteria in such a way as to minimize the contribution of single-pion exchange and the effects of final-state resonant interactions in the $p_f\pi^-$ system. We chose events with large momentum transfer to the neutron, $|t_{p_s}| \geq 0.4$ $(\mathrm{GeV}/c)^2$ and with large $p_f\pi^-$ effective-mass $M(p_f\pi^-) \geq 1.8$ GeV/c^2. In Figs. 4 (a) and 4 (b) we show, for the 229 events selected according to these requirements, the $M(p_s\pi^-)$ and t_{p_f} distributions respectively. These show a peak near 1470 MeV/c^2 in the mass distribution and give evidence for peripheral production. For the 104 events with 1.32 $\mathrm{GeV}/c^2 \leq M(p_s\pi^-) < 1.60$ GeV/c^2, we show the distributions in momentum transfer as the shaded histogram of Fig. 4 (b) and in cosine of scattering angle $\cos\theta_{p_s}$ as the unshaded histogram in Fig. 4 (c). Further restriction to peripheral production, $|t_{p_f}| < 0.4$ $(\mathrm{GeV}/c)^2$ results in a sample of events with distributions in $M(p_s\pi^-)$ displayed in the shaded histogram in Fig. 4 (a), and in $\cos\theta_{p_s}$ displayed, cross-hatched, in Fig. 4 (c). Fits to the momentum transfer distributions shown in Fig. 4 (b), to the form $ce^{-\alpha t}$ yield slopes $\alpha = 6.4 \pm 1.1$ $(\mathrm{GeV}/c)^{-2}$ for the complete sample and $\alpha = 7.5 \pm 1.5$ $(\mathrm{GeV}/c)^{-2}$ for the events with restricted $M(p_s\pi^-)$ values. In making the fits, only those data with $0.08 \leq |t_{p_f}| < 0.4$ $(\mathrm{GeV}/c)^2$ in the upper histogram and with $|t_{p_f}| < 0.4$ $(\mathrm{GeV}/c)^2$ in the shaded were considered. These slopes may be compared with the value $\alpha = 20.7 \pm 2.7$ $(\mathrm{GeV}/c)^{-2}$ obtained by Blair et al.[1] for anomalous N* (1400) production observed with a massing-mass spectrometer.

Since the characteristics of these events are not qualitatively very much different from the peripheral ($|t_{p_s}| < 0.4$ $(\mathrm{GeV}/c)^2$) data discussed above, a straightforward application of the single pion exchange model was made here also. The theoretical expression used for the events with $|t_{p_s}| \geq 0.4$ $(\mathrm{GeV}/c)^2$, where the model is of questionable validity perhaps, differed from that described above in the exclusion of the phenomenological form-factor (7)[13]. Using the Monte-Carlo technique to generate events and applying the same restrictions as to the data, there resulted the various curves drawn in Fig. 4.

The solid curves in Fig. 4 are normalized to the total number of events and the dashed curve in Fig. 4 (b) is to be compared with the cross-hatched histogram of the restricted sample with $1.32 \text{ GeV}/c^2 \leq M (p_s\pi^-) < 1.60 \text{ GeV}/c^2$. The dependence of the data on the momentum transfer t_{p_f} is less steep than the model predictions. In addition, the mass distributions in Fig. 4 (a) are not well represented by the model, although the discrepancies are not severe, considering the limited statistical accuracy. This is particularly so for the lower momentum transfer data. The angular distribution of Fig. 4 (c) is in good agreement with the model's predictions. Conceding the doubtful applicability of the model to the events with $|t_{p_s}| \geq 0.4 \text{ (GeV/c)}^2$, we may consider its predictions to phenomenologically represent the shape of the background to be subtracted from the $M (p_s\pi^-)$ distribution. Taking this point of view, we make the generous estimate of thirty five events to be attributed to N* (1470) production by some unspecified mechanism. Events with $|t_{p_s}| \geq 0.4 \text{ (GeV/c)}^2$ and $M (p_f\pi^-) < 1.8 \text{ GeV}/c^2$ show a smooth variation with $M (p_s\pi^-)$ and so provide a contribution of not more than five resonance-production events. At most five percent of the data may then be attributed to N* (1470) production, by some mechanism other than pion-exchange, about a factor ten smaller than that reported by Shapira et al at 7 GeV/c incident momentum.

The results reported here were made possible by the usual high quality performance of the Bevatron and Bubble Chamber, for which we thank the operating crews. The continued support of Professor E. Segrè and initial assistance of Professors P. Condon, M. Mandelkern and J. Schultz are gratefully acknowledged.

REFERENCES AND FOOTNOTES

* Supported by the United States Atomic Energy Commission

(1). C. M. Ankenbrandt et. al., Nuovo Cimento 35, 1052 (1965), G. Belletini et. al. Physics Letters 18, 167 (1965), E. W. Anderson et. al. Phys. Rev. Letters 16, 855 (1966), I. M. Blair et. al. Phys. Rev. Letters 17, 789 (1966), K. J. Foley et. al. Phys. Rev. Letters 19, 397 (1967).

(2). L. D. Roper, Phys. Rev. Letters 12, 340 (1964); L. D. Roper, R. M. Wright and B. T. Feld, Phys. Rev. 138, B190 (1965); L. D. Roper and R. M. Wright, Phys. Rev. 138, B921 (1965); For the recent status of the results from πN phase shift analyses, see A. Donnachie, *Proceedings of the Fourteenth International Conference on High Energy Physics*, Vienna, Austria, (September, 1968). p. 139.

(3). A. Shapira, O. Benary, Y. Eisenberg, E. E. Ronat, D. Yaffe, and G. Yekutieli, Phys. Rev. Letters 21, 1835 (1968).

(4). L. Hulthén and M. Sugawara in *Haudbuch der Physik* (Springer-Verlag, Berlin, (1957), Vol. 39, Chapter 1).

(5). See, e. g., R. G. Newton, *Scattering Theory of Waves and Particles*, (McGraw-Hill, 1966), Chapter 8.

(6). H. P. Dürr and H. Pilkuhn, Nuovo Cimento 40, 899 (1965).

(7). G. F. Chew and F. E. Low, Phys. Rev. 113, 1640 (1959).

(8). G. Wolf, Phys. Rev. Letters 19, 925 (1967).

(9). E. Colton, P. E. Schlein, E. Gellert and G. A. Smith, University of California, Los Angeles, Report No. UCLA-1023 Rev., presented at the XIV International Conference on High Energy Physics, Vienna, Austria (September, 1968).

(10). E. Colton, S. Prum, P. E. Schlein, and A. J. Verglas, Nuclear Physics B17, 117 (1970).

(11). This parameterization of the form factor G (t) was introduced by G. Goldhaber et al, Physics Letters 6, 62 (1963).

(12). A. Donnachie, R. G. Kirsopp and C. Lovelace, CERN Th. 838 Addendum (phase shifts), (1967).

(13). G. Wolf, Phys. Rev. 182, 1538 (1969). The Dürr-Pilkuhn form factors predict a too-rapid decrease for large values of t. We thus empirically flatten the predicted t dependence by simply removing the additional form factor G (t).

FIGURE CAPTIONS

Fig. 1. Fitted distributions of (a) spectator momentum and (b) cosine of the angle between the spectator and incident proton directions in the laboratory system. The smooth curves are Hulthén distributions with $\beta = 5.18\ \alpha$, normalized to the total number of 904 $pd \rightarrow pp\pi^- p_{sp}$ events; the Möller flux-factor is taken into account.

Fig. 2. Distributions of four-momentum transfer squared from (a) initial neutron to final slower proton p_s and (b) initial proton to final faster proton p_f; effective mass of (c) $p_f\pi^-$ system and (d) $p_s\pi^-$ system. In (b) - (d) the shaded histograms are for events with $|t_{p_s}| < 0.4\ (GeV/c)^2$. The curves give the predictions of a single-pion exchange model whose details are discussed in the text.

Fig. 3. Distributions, for events with $|t_{p_s}| < 0.4\ (GeV/c)^2$, of (a) $\cos\theta_{p_f}$, where θ_{p_f} is the angle between the incident proton and outgoing faster proton evaluated in the $p_f\pi^-$ rest system, (b) $\cos\theta_{p_s}$ where θ_{p_s} in the angle between the initial neutron and final slower proton; (c) Treiman-Yang angle Φ_{p_f}, the azimuthal angle of p_f in the $p_f\pi^-$ rest frame, (d) Treiman-Yang angle Φ_{p_s} in the $p_s\pi^-$ rest frame; momentum-transfer squared (e) $t_{p\pi^-}$ from the initial proton to the π^- and (f) $t_{n\pi^-}$ from the initial neutron to the π^-. The curves give the predictions of a single-pion exchange model discussed in the text.

Fig. 4. Distributions of events with the restrictions $M(p_f\pi^-) \geq 1.8\ GeV/c^2$ and $|t_{p_s}| \geq (0.4\ GeV/c)^2$. (a) Effective mass of the $p_s\pi^-$ system; the shaded distribution represents events with $|t_{p_f}| < 0.4\ (GeV/c)^2$. (b) Four-momentum transfer squared, $|t_{p_f}|$; the shaded distribution represents events with $1.32\ GeV/c^2 \leq M(p_s\pi^-) < 1.60\ GeV/c^2$. (c) $\cos\theta_{p_s}$ for events with $1.32\ GeV/c^2 \leq M(p_s\pi^-) < 1.60\ GeV/c^2$; the events in the shaded histogram have, in addition, $|t_{p_f}| < 0.4\ (GeV/c)^2$. The curves give the predictions of the single-pion exchange model discussed in the text.

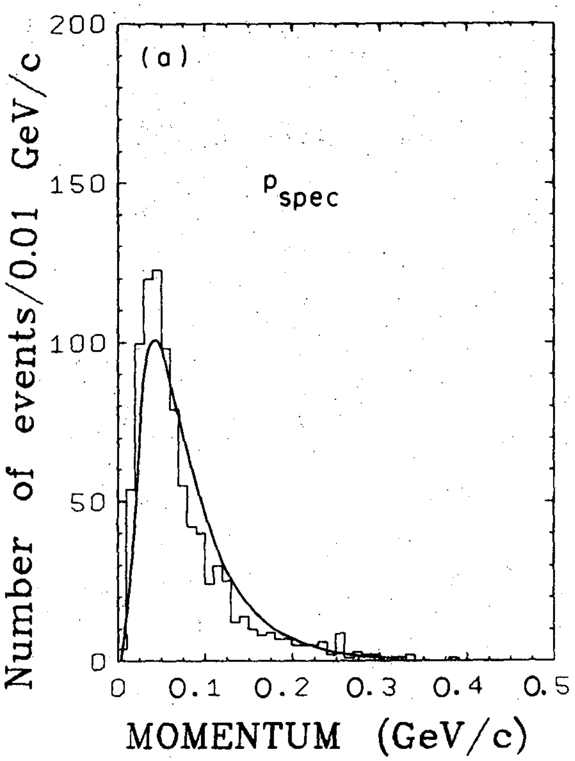
(a)
p_{spec}
Number of events/0.01 GeV/c
MOMENTUM (GeV/c)
0
50
100
150
200
0
0.1
0.2
0.3
0.4
0.5

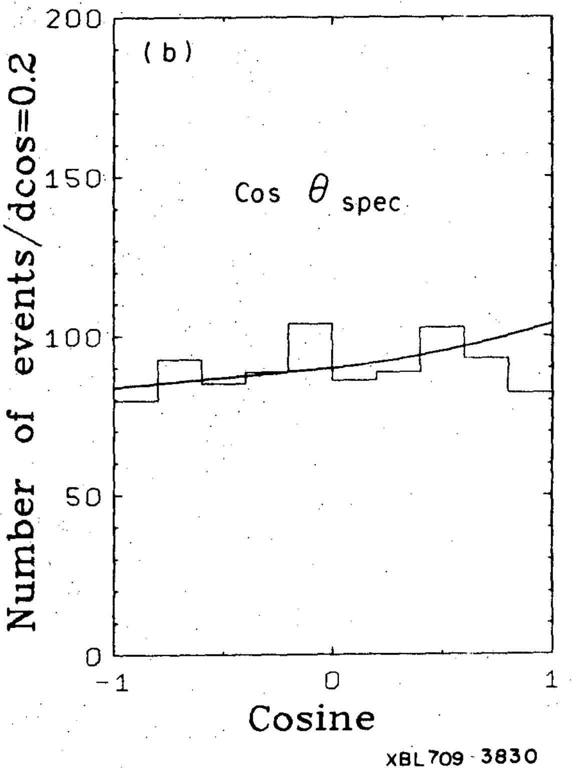
(b)
Cos θ_{spec}
Number of events/dcos=0.2
Cosine
0
50
100
150
200
−1
0
1
XBL709-3830

FIGURE 1

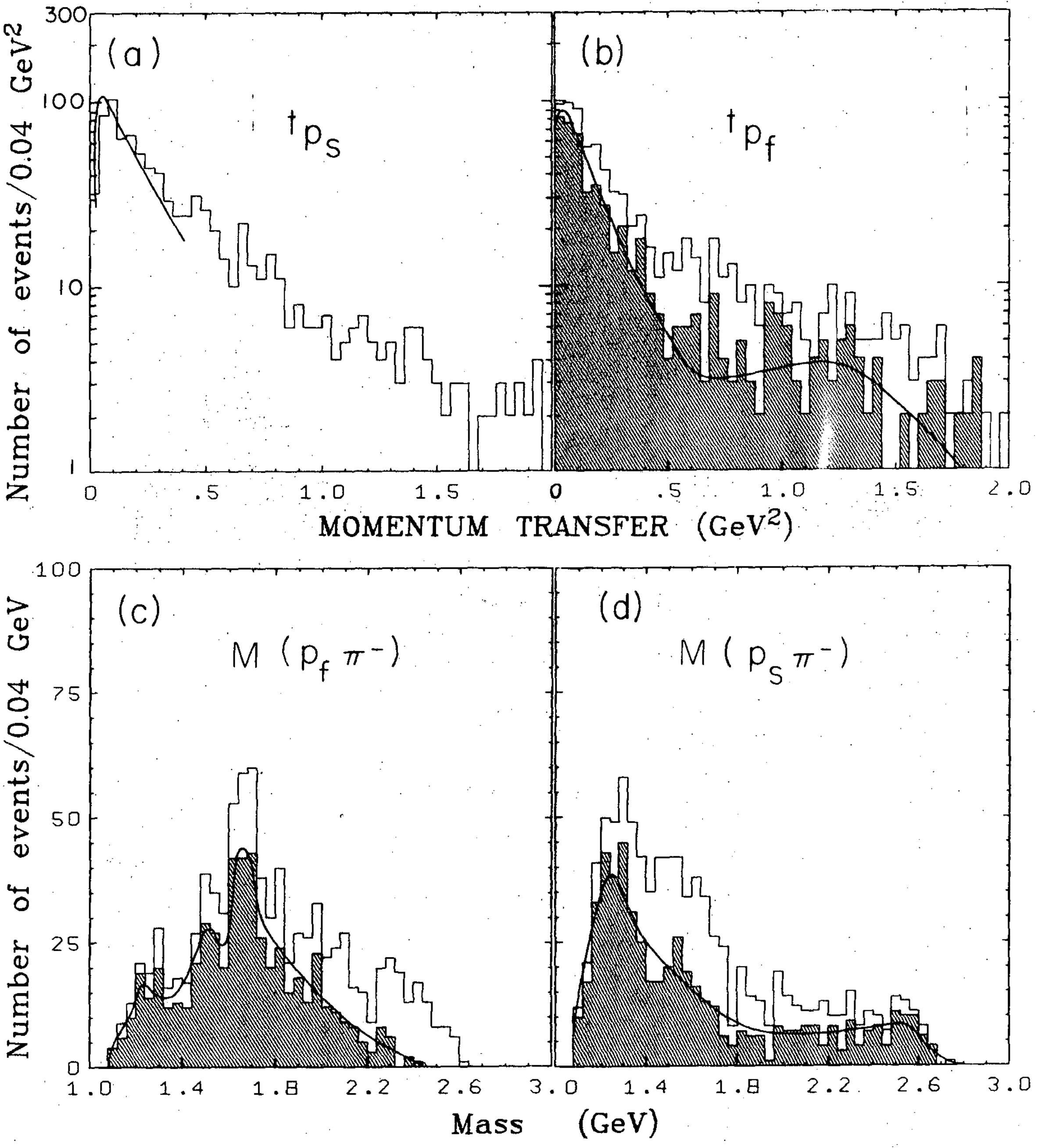

XBL709-3831

FIGURE 2

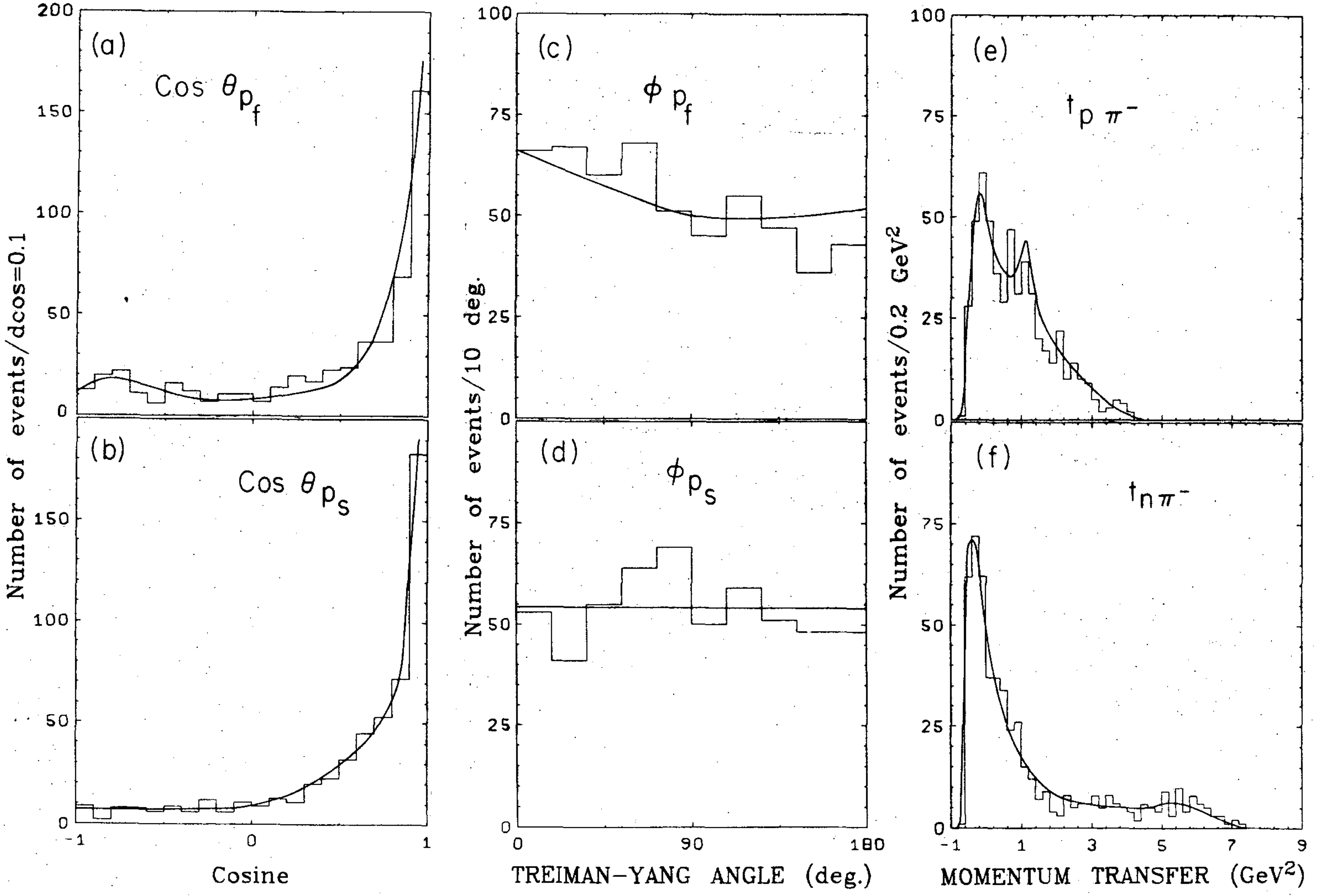

XBL 709-3827

FIGURE 3

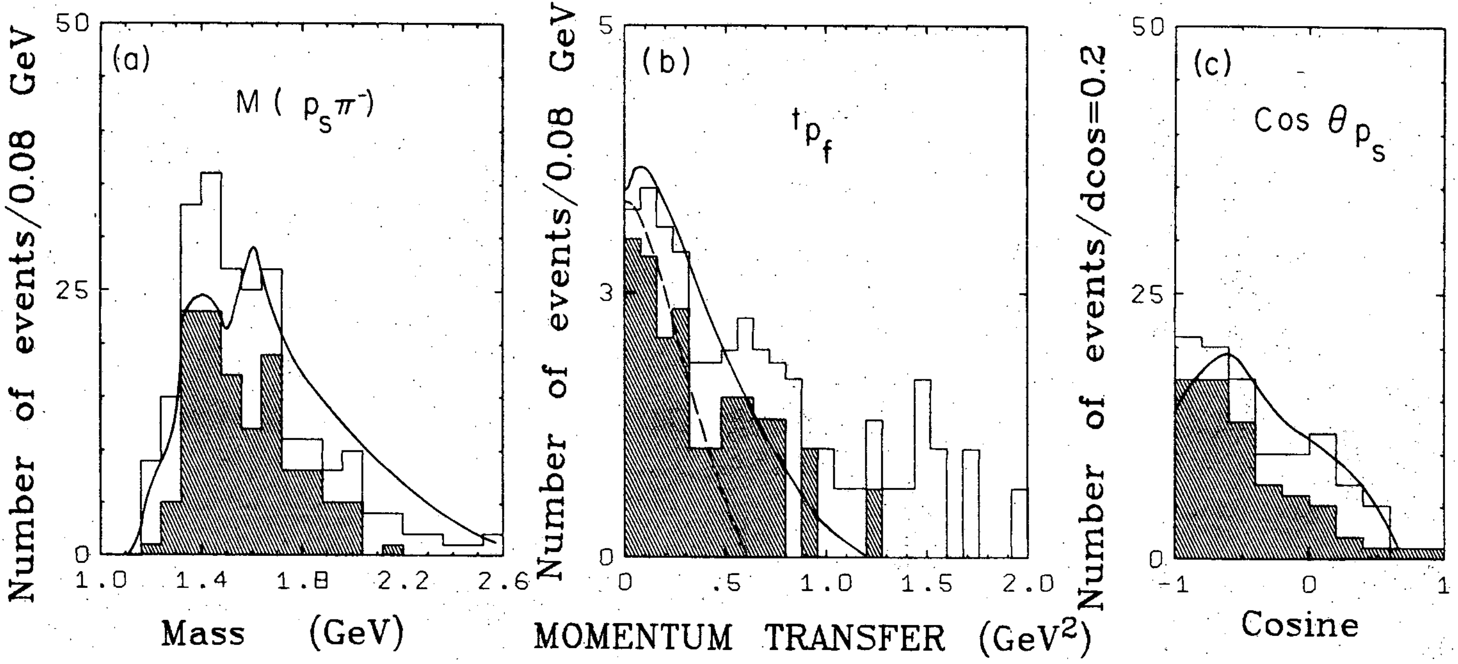

XBL709-3829

FIGURE 4

TECHNICAL INFORMATION DIVISION
LAWRENCE RADIATION LABORATORY
UNIVERSITY OF CALIFORNIA
BERKELEY, CALIFORNIA 94720